

University of Mississippi

eGrove

Electronic Theses and Dissertations

Graduate School

2016

Biophysical Characterization Of A Proline Mutant Of Neural Cadherin

Keshia S. Dykes

University of Mississippi

Follow this and additional works at: <https://egrove.olemiss.edu/etd>



Part of the [Chemistry Commons](#)

Recommended Citation

Dykes, Keshia S., "Biophysical Characterization Of A Proline Mutant Of Neural Cadherin" (2016). *Electronic Theses and Dissertations*. 921.

<https://egrove.olemiss.edu/etd/921>

This Thesis is brought to you for free and open access by the Graduate School at eGrove. It has been accepted for inclusion in Electronic Theses and Dissertations by an authorized administrator of eGrove. For more information, please contact egrove@olemiss.edu.

BIOPHYSICAL CHARACTERIZATION OF A PROLINE MUTANT OF NEURAL
CADHERIN

A Thesis
presented in partial fulfillment requirements
for the degree of Master of Science
in the Department of Chemistry and Biochemistry
The University of Mississippi

by

KESHIA S. DYKES

MAY 2016

Copyright Keshia S. Dykes 2016
ALL RIGHTS RESERVED

ABSTRACT

Cadherins are calcium dependent glycoproteins whose homophilic interactions mediate cell-cell adhesion in solid tissues. They are comprised of an extracellular region, a transmembrane region and a cytoplasmic region. The extracellular region plays a critical role in cadherin-mediated cell adhesion, and has five tandemly repeated ectodomains (EC1-EC5), with three calcium binding sites situated in each interface between the domains. Dimerization of cadherin occurs through formation of adhesive interactions between extracellular domains of cadherins from neighboring cells. Adhesive interaction occurs at the interfaces of EC1 domains of two molecules originating from different cell surfaces. Dimerization is critically dependent on the binding of calcium. Neural and epithelial cadherin (NCAD and ECAD) are very similar in sequence comparison, but differ in kinetics of dimer assembly and dimer affinity in the presence or absence of calcium. The single most obvious difference in the strand swapped interface is a proline in NCAD and a glutamate in ECAD in position 16. Our hypothesis is that the slow kinetics of dimer disassembly of NCAD is due to the steric restrictions of proline in position 16 of NCAD. The purpose of this research is to mutate the proline, in position 16 to alanine (P16A), in NCAD to decrease the steric hindrance and study the effects of the mutation. Stability studies assess the effect the mutation has on the folding properties of the protein. Calcium binding experiments demonstrate whether the mutation affects the binding affinity of calcium. From the results, P16A lowers the stability of the protein, Ca²⁺ binding affinity, and dimerization kinetics of NCAD.

DEDICATION

This thesis is dedicated to my family, who encouraged, prayed and supported me during this journey. I love you Mom, Dad, Granny Teate, Carrie, Kieon, and CJ.

LIST OF ABBREVIATIONS AND SYMBOLS

NCAD	Neural Cadherin
ECAD	Epithelial Cadherin
P16A	Proline in 16th position mutated to Alanine in NCAD
Pro16	Proline in the 16 th position in NCAD
R14	Arginine in 14th position in NCAD
R14S	Arginine in 14th position mutated to Serine in NCAD
R14A	Arginine in 14th position mutated to Alanine in NCAD
R14E	Arginine in 14th position mutated to Glutamate in NCAD
K14	Lysine 14th position in ECAD
D138	Aspartate in 138th position
Apo	Calcium-depleted
CD	Circular dichroism
FL	Fluorescence
EC	Extracellular domain
EC1	Extracellular domain 1 of NCAD12
EC2	Extracellular domain 2 of NCAD12
EDTA	Ethylenediaminetetraacetic acid
HEPES	N-(2-hydroxyethyl) piperazine-N'-2-ethanesulfonic acid
K _a	Acid Dissociation Constant;
K _d	Dissociation constant;

NaOAc	Sodium Acetate
NCAD12	Neural-cadherin extracellular domains 1 and 2 (residues 1 to 221)
ECAD12	Epithelial-cadherin extracellular domains 1 and 2 (residues 1 to 213)
PAGE	Polyacrylamide gel electrophoresis
SEC	Size exclusion chromatography
T _m	Melting temperature
aa	Amino acids

ACKNOWLEDGMENTS

I would like to thank each individual who impacted my life to make this journey memorable. Through their encouragement and kind words, I was able to continue to strive for excellence and complete my thesis project.

I would like acknowledge my advisor, Dr. Susan Pedigo and my committee members, Dr. Watkins and Dr. Cleland. Also, I would like to thank Dr. Shana Stoddard, Mrs. Harriet, Mrs. Michelle, Mrs. Sirena, and the staff and faculty of the University of Mississippi Department of Chemistry and Biochemistry. I learned many life lessons from them and I am greatly thankful for their impact, support, and encouragement.

Finally, I would like to thank my family, mentors, and friends. These individuals continued to support me academically, spiritually and mentally. I am entirely grateful for their unconditional love and generous support through my thesis process.

Additionally, I would like to acknowledge Victoria McClearn who assisted in some of the preliminary work.

TABLE OF CONTENTS

ABSTRACT	ii
DEDICATION	iii
LIST OF ABBREVIATION AND SYMBOLS	iv
ACKNOWLEDGEMENTS	vi
LIST OF TABLES	viii
LIST OF FIGURES	xi
CHAPTER 1: INTRODUCTION	1
CHAPTER 2: METHODS AND MATERIALS	10
CHAPTER 3: RESULTS	15
CHAPTER 4: DISCUSSION	24
BIBLIOGRAPHY	28
VITA	34

LIST OF TABLES

Table 1: Sequence comparison of NCAD12 and ECAD12	4
Table 2: Resolved parameters of Thermal Denaturation	20
Table 3: Free Energies of Calcium Binding Resolved from Analysis of Calcium	23

LIST OF FIGURES

Figure 1: General cadherin structure showing the extracellular region, transmembrane region and a cytoplasmic region	2
Figure 2: Calcium Dependent Strand Swapped Dimer Mechanism	5
Figure 3: Proline and alanine	9
Figure 4: 17% SDS-PAGE of Protein Expression and Purification	16
Figure 5: Thermal Denaturation of NCAD12	18
Figure 6: Thermal Denaturation of NCAD12 P16A	19
Figure 7: Calcium Titration through Fluorescence Spectrometry	21
Figure 8: Calcium Titration through Circular Dichroism	22

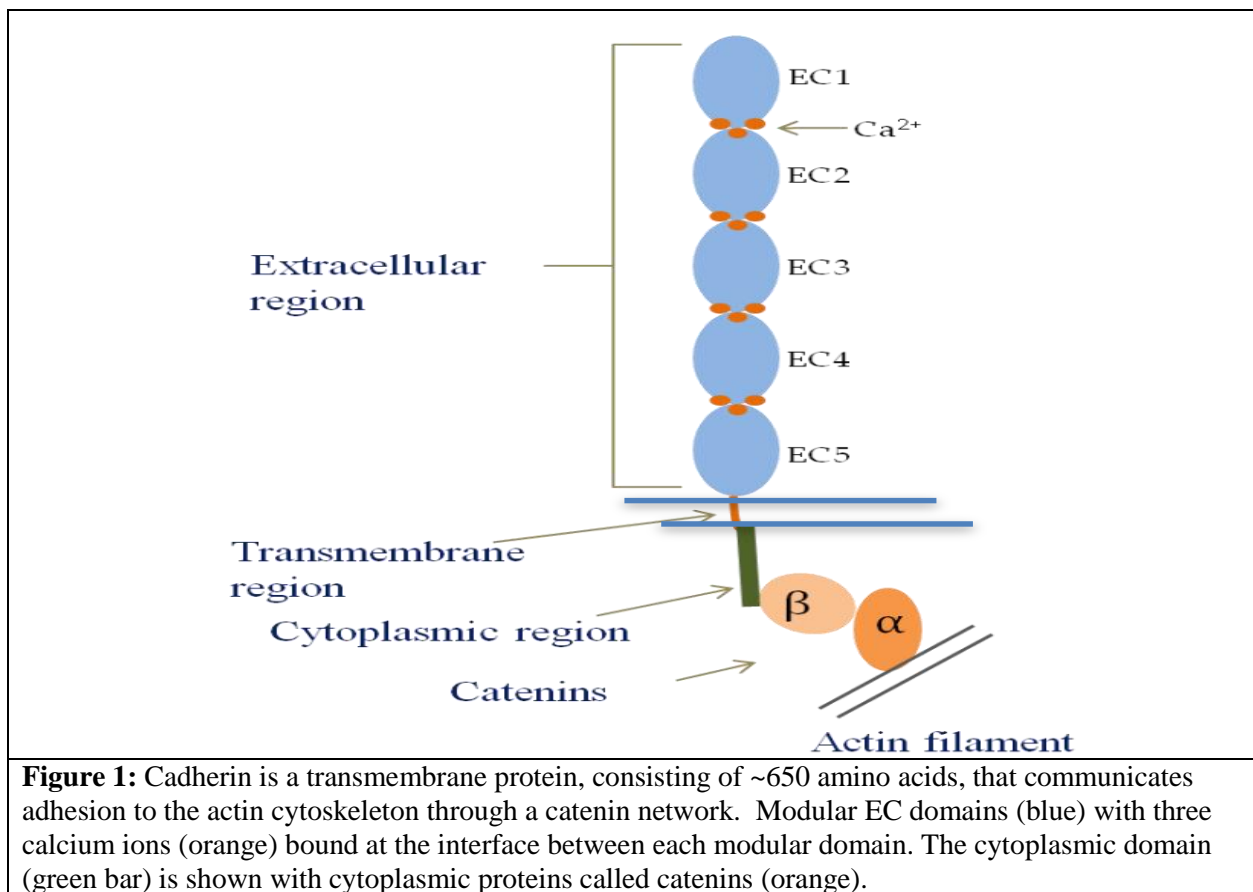
CHAPTER I

INTRODUCTION

Cell adhesion is the interaction that occurs between cell surfaces and the extracellular matrix which enables development, formation, and maintenance of tissues in multicellular organisms. In addition, for tissues to form properly, cells must adhere to other cells in an organized fashion. In order for cell-cell adhesion to occur in adherens junctions, tight junctions, and desmosomes, cell-cell adhesion transmembrane proteins are required. Most cell adhesion molecules are transmembrane glycoproteins belonging to one of these five families: cadherins, mucins, integrins, selectins, and immunoglobins. These families are either calcium dependent or independent molecules and have specific functions for cell adhesion ¹⁻³.

Classical cadherins are calcium dependent glycoproteins whose homophilic interactions mediate cell-cell adhesion in solid tissues⁴. Cadherins are responsible for maintaining the integrity of multicellular tissues, selecting cell-cell adhesion (cell sorting), and playing important roles in embryogenesis ⁵⁻⁹. Any abnormalities can affect long term potentiation and synapse duration. Regarding metastasis of cancer, cadherin dysfunction occurs through genetic mutations, low expression, and changes in the tumor microenvironment ¹⁰⁻¹⁴. Because of the importance of cadherin in normal tissue function and maintenance, research in our laboratory is focused on understanding the molecular basis of cadherin function. We use biophysical approaches to study the linkage between calcium binding and dimerization equilibria and kinetics in neural- and epithelia-cadherins, the two most prominent members of the classical cadherin family.

Cadherins have a similar structure comprised of three parts: an amino-terminal extracellular region, a transmembrane segment, and a conserved carboxyl terminal intracellular region **Figure 1**. The extracellular region consists of five extracellular domains (EC1-EC5), approximately 100 amino acid residues each. Cadherins allow adherent cells to communicate due to tension communicated through cadherin EC domains to the cytoplasmic domain. The C-domain of cadherin is connected to the actin cytoskeleton through the catenin network. Each EC domain has seven (A-G) antiparallel β -strands. Between successive EC domain is an interface which binds three calcium ions ¹⁵⁻¹⁶.



NEURAL AND EPITHELIAL CADHERIN

Type I or classical cadherins are located in adherens junctions and are named according to the cell type in which they predominate. Neural cadherin (NCAD) and epithelial cadherin (ECAD) are the most studied members of the cadherin family. They are very similar in sequence and structure, but have different dimerization affinity and kinetics. While ECAD is the predominant classical cadherin in epithelial cells, like NCAD, it is also located in the central nervous system. These two cadherins can be expressed in the same neuron at different synapses. ECAD is found in inhibitory synapses and NCAD in excitatory synapses. Inhibitory synapses contain a relatively constant calcium concentration and are located in dendritic shafts, soma, and proximal axonal regions of neurons¹⁷⁻¹⁸. Excitatory synapses are located in dendritic spines and the calcium concentration fluctuates depending on the signaling event. Their localization at distinct synapses indicates they have unique applications. Altered metabolism of N-cadherin results in synaptic dysfunction, a primary feature of Alzheimers disease⁴⁰. In addition to their neurological roles, abnormal expression of N-cadherin by carcinoma cancer cells can contribute to invasiveness and metastasis by making the cells more motile³⁸⁻³⁹.

SEQUENCE

NCAD12 and ECAD12 have a very similar amino acid sequence with only a few differences. These differences may play a vital role in monomer-dimer equilibrium. The EC1 and EC2 domain sequences for both proteins were aligned using LALIGN¹⁹ (**Table 1**). Based on this program, ECAD12 and NCAD12 have a highly conserved level of sequence homology. The comparison sequence shows that EC1 domain is 57% identical and 27% similar, linker 1 region is 86% identical and 14%, similar, EC2 domain is 54% identical and 23% similar, and linker 2 region is 71% identical and 29% similar. Overall, these 2-domain constructs are 81% identical or similar.

of calcium rigidifies the linker regions between successive domains into a proper orientation ($\sim 90^\circ$), and maintains the overall domains in certain conformational flexibility as well ²⁴.

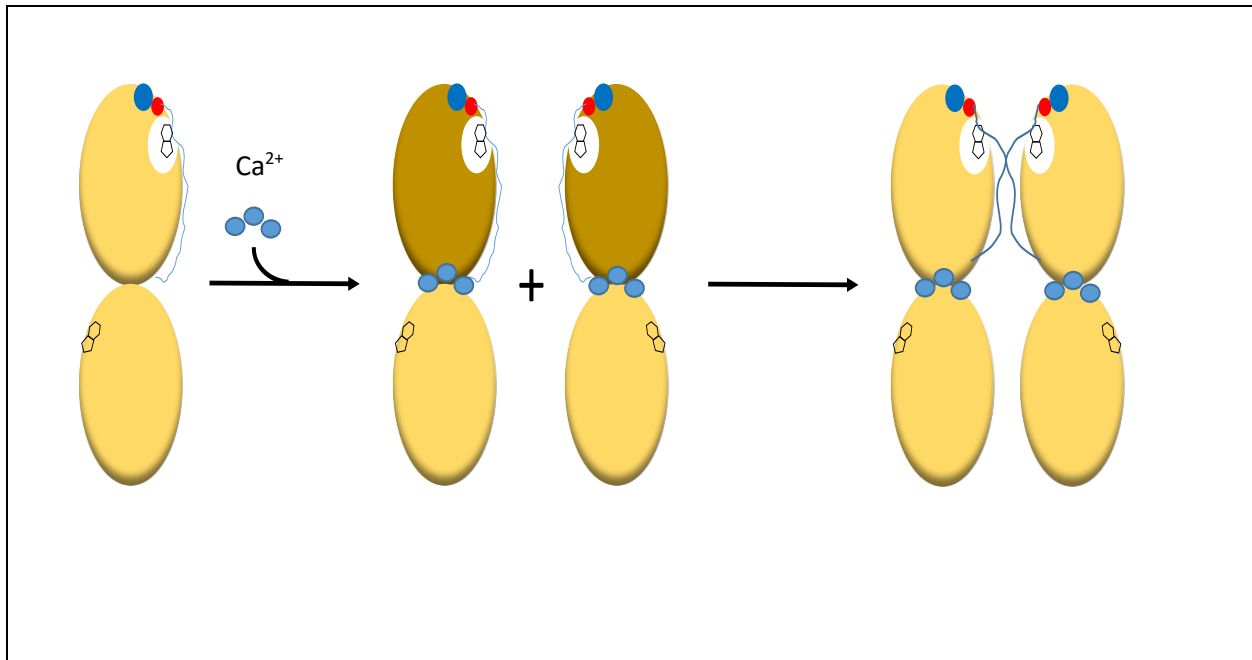


Figure 2: Calcium-dependent Strand-Swap Dimer Mechanism. The apo monomer consists of domains EC1 and EC2 without the presence of calcium. W2 on β A strand is docked into its own hydrophobic pocket. When three calciums are added between domains EC1 and EC2, it causes a conformational strain in the “closed” Ca²⁺ saturated monomer (darker EC1). To relieve this strain, the W2 β A strand docks into the neighboring monomer’s hydrophobic pocket. Thus, creating the strand-swap dimer.

As described above the extracellular domains of classical cadherin interact through direct noncovalent interactions: ionic interaction, hydrophobic interactions, and hydrogen bonding. The strand-swapped adhesive interaction occurs at the interfaces of EC1 domains of two molecules originating from different cell surfaces, and as such is called a trans dimer. The lateral interaction is another type of dimerization. It occurs between the interface of EC1 domain of molecule A and EC2 domain of molecule B in a parallel orientation from the same cell surface. The “front-to-back” contacts are called lateral or cis interfaces because the protomers come from the same cell. A hydrophobic surface on the “back” of EC1, away from the site of strand exchange, interacts with a hydrophobic region at the bottom of EC2. Lateral interactions have been observed

in N-, E- and C- cadherin molecules in crystal structures, but do not always agree in this form⁴²⁻⁴⁴. The data were entirely structural and there was no corroborating biological evidence⁴⁵. Ozawa et al used an immunoprecipitation approach to analyze lateral dimer formation by E-cadherin. Yet, Ozawa reported that the lateral dimerization was not sufficient for adhesive activity⁴¹. Thus, the functional significance of lateral interactions is still debated because the formation of lateral dimers is extremely low affinity under in vitro conditions.

DIMERIZATION KINETICS

Both NCAD and ECAD form adhesive dimers through the mutual exchange of the β A strand, but differ in dimerization kinetics. NCAD (25 μ M) dimerization affinity is four times higher than ECAD (100 μ M)²⁰. Studies have shown that ECAD forms dimer that is in rapid exchange with monomer with or without the presence of calcium. NCAD also forms dimer in rapid exchange with monomer in the presence of calcium. However, in the absence of calcium there is very slow monomer dimer exchange in NCAD such that a kinetically trapped dimer is formed²⁵. To explain the rapid exchange between monomer and dimer in ECAD, a low affinity dimeric intermediate structure called “X-dimer” was proposed²⁶. X-dimer (also called the initial encounter complex) is a transition state complex that functions as an intermediate structure between monomer and the strand swapped dimer. The closed monomer state has its W2 buried into its own hydrophobic pocket. The closed dimer state is the strand-swapped dimer in which EC1 domains of the two interacting protomers are in direct contact. W2 residues are docked inside of their partner’s hydrophobic pocket. EC2 domains are not in direct contact. To form the closed dimer, β A-strand of each protomer must open by breaking noncovalent forces before reforming them in the adhesive dimer partner. In both states, the closed monomer and closed dimer, the W2s are not exposed to solvent⁴⁶ and are either docked inside their own or their partner’s hydrophobic cleft. Therefore,

forming an initial-encounter complex is necessary to keep the β A-strand buried either in closed monomer form or in closed dimer form. Meanwhile, forming an X-dimer lowers the activation barrier of assembly and disassembly of dimers.

Harrison's X-dimer model for ECAD drew special attention to lysine 14 as a key player in the stabilization of the X-dimer intermediate. NCAD and ECAD both have a basic amino acid at position 14, and are positively charged. In ECAD, K14 interacts with D138 on the opposing protomer which interacts in the X-dimer. Beyond the apparent importance of K14 in the structural data, its function was studied with the K14 to glutamate mutant (K14E). This mutant showed very slow kinetics of dimerization with no apparent effect upon the dimerization affinity²⁸.

In NCAD, there is no structural data to support the role for R14 interactions in the rapid kinetics of dimerization of NCAD in the presence of calcium. Kinetics studies were performed to investigate the role of R14 in the rapid dimerization of NCAD with and without calcium²⁷⁻²⁸. Several mutants (arginine mutated to serine R14S, glutamate R14E, and alanine R14A) were prepared with "X-dimer" forming capabilities. The loss of R14 did not slow dimerization unless it was mutated to glutamate, which drastically slowed down dimerization in the presence of calcium.

Because mutation of the basic residue in position 14 to an acid residue has a profound effect on the dimerization kinetics of ECAD and NCAD, interest has been placed on the dimerization interface region, which is roughly amino acids 10-18 in the sequence of ECAD and NCAD, as an important contributor to dimerization kinetics. In that particular region, there happens to be several prolines in positions 10, 16, and 18. However, the prolines in position 10 and 18 are conserved in both sequences (ECAD and NCAD). Only the proline in position 16 is different. This proline at position 16 could be the reason for the slow dimerization in NCAD. The purpose of this research

is to mutate the proline in position 16 to an alanine (P16A), to decrease steric hindrance, and study the kinetic effects.

PROLINE

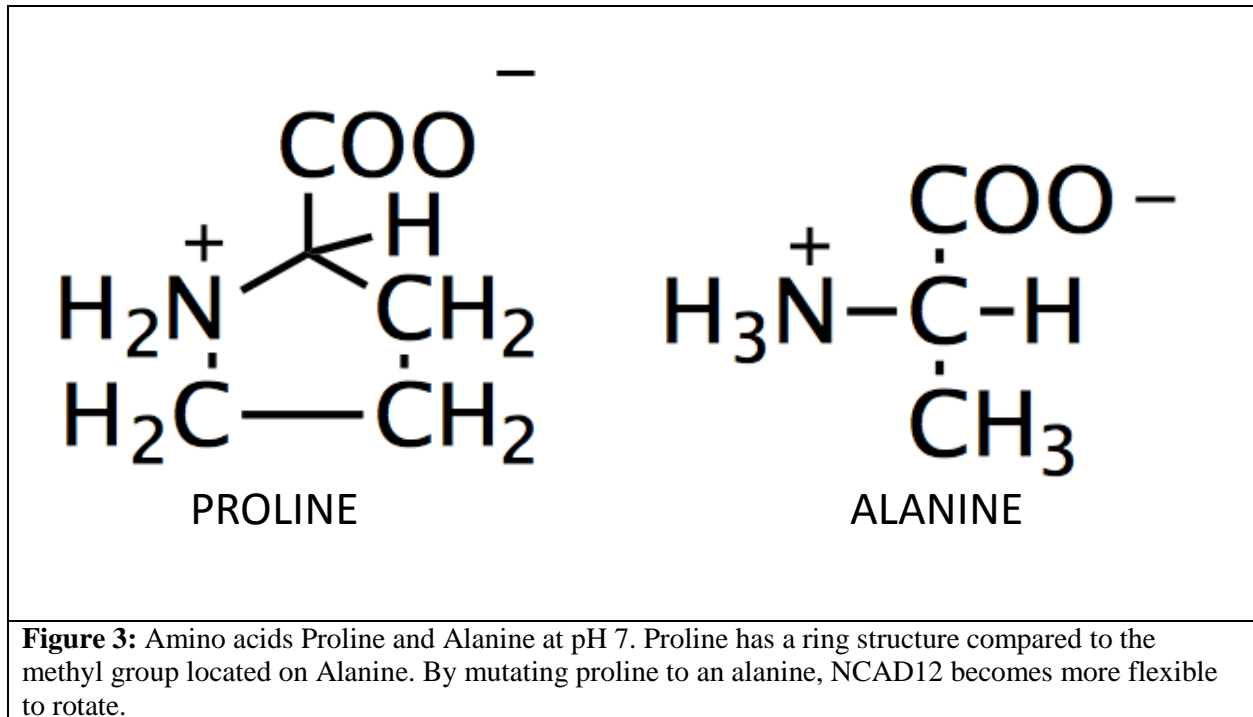
Proline has intrinsic roles in protein function and stability. Proline is the only amino acid where the side chain is directly connected to the protein backbone in two places, α -C and amide N. As such, proline is a secondary amine, forming a five-membered nitrogen-containing ring. Often proline is found in β turns in proteins, structures that are known to be evolutionarily conserved²⁹. X-pro peptide bonds exist in cis and trans configurations. The trans configuration is preferred over the cis because there is less steric hindrance between the amide hydrogen and the previous α carbon. Conversely, the cis configuration becomes more prevalent as the solvent becomes more polar³⁰. In native proteins that contain X-pro bonds, prolines are either completely cis or trans configuration. Isomerization of these conformations can be slow and be the rate determining step in protein folding.

There have been many studies demonstrating the critical roles of prolines. Green et al. showed that deletion of six amino acids in a surface loop converted a monomeric protein into a stable dimer³¹. Findings by Baldwin et al. demonstrated that mutation of two prolines in cis pro bonds, 93 and 114, in Ribonuclease A destabilized the protein³². Likewise, Marqusee et al. argued that proline 114, in Ribonuclease A, facilitates domain swapping³³. In our lab, it has been shown that mutating two prolines, positions 5 and 6 in NCAD, were necessary for stabilizing the dimer relative to the monomer to promote dimerization³⁴⁻³⁵.

SCOPE OF WORK

It has already been stated that proline plays a vital role in protein folding and stability and dimer assembly. Proline can be easily substituted for other small amino acids using site-directed

mutagenesis of the gene that codes for the protein. The purpose of this research is to mutate proline16 to alanine (P16A), in NCAD12 to decrease the steric hindrance and study the effects of the mutation on the structure and function of NCAD12. Stability studies assess the effect the mutation has on the folding and stability of the protein. Calcium binding experiments demonstrate whether the mutation affects the binding affinity for calcium.



CHAPTER II

METHODS AND MATERIALS

PROTEIN EXPRESSION

For the expression of NCAD12-P16A (P16A), LB agar plates and LB agar plates with a Kanamycin (Kan) resistant had to be prepared. These plates were prepared in two 250 ml Erlenmeyer flasks by mixing 100 ml water, 2.0 g tryptone, 1.0 g yeast extract, 1.0 g NaCl, and 1.5 g agar. The solutions were covered with aluminum foil, labeled, taped with autoclave tape, and autoclaved. Once the solutions were autoclaved, they cooled on the benchtop at room temperature until they reached 55°C. To one flask, 100 ul of Kan stock (100 ug/ml) was added. Labeled plates (LB or LB/Kan) were poured with the appropriate solution (LB or LB/Kan) and allowed to solidify overnight on the benchtop at room temperature. The next day all plates were parafilmed and stored in the refrigerator until needed. A sample of NCAD12-P16A expression cell line was taken from the -80°C freezer. With a sterile inoculating loop, NCAD12-P16A expression line *E.coli* cells (BC21-DE3) were streaked on a LB/Kan plates. The plates were incubated overnight at 37°C and checked for colony growth the next day. A 50 ml liquid media solution, in a 250 ml Erlenmeyer flask, was prepared similar to LB/Kan agar except no agar was added. The solution cooled, then a colony was chosen from the streaked plate and used to inoculate the media as the overnight culture. The culture was placed in the incubator overnight at 37°C and rotated at 200 rpm. In two 2.5 L Fernbach flasks, the large expression culture, 1 L sterile LB was prepared. Each flask contained 1 L water, 20 g tryptone, 10 g yeast extract, and 10 g NaCl. The solutions were covered with

aluminum foil, labeled, taped with autoclave tape, and autoclaved. Once the solutions were autoclaved, they cooled on the benchtop until they reached 55°C. A volume of 1 mL of Kan stock was added to each flask. The solutions cooled on the benchtop overnight at room temperature. To each flask, 15 mL of 20% glucose, 37.5 mL of 1M-potassium phosphate and 5 mL of overnight culture were added. These large expression cultures were placed in the incubator for three hours at 37°C and rotated at 200 rpm. After the three hours the absorbance was checked at 600 nm and blanked against the LB only media. The absorbance was checked every 15 minutes in order to accurately identify the 0.5 AU induction period. Once the A_{600} is near ~0.3 AU, the growth rate rapidly increases. After four hours, the cultures were induced at A_{600} 0.4526. A volume of 1 mL of IPTG was added to induce each culture. The cultures were incubated and grown for two hours at 37°C and rotated at 200 rpm. The liquid cultures were transferred to 1L bottles and centrifuged at 4°C at 3000 rpm for 20 minutes. The supernatant was decanted and a pellet remained in the bottle. The pellet was re-suspended using 10 mL of 20 mM HEPES, 100 mM KCl, pH 7.4 buffer. Then, the solution was frozen at -20°C.

PROTEIN PURIFICATION

The frozen solution was thawed, then sonicated to lyse the cells and release the protein. The cells were centrifuged at 13,000 rpm and 4°C for 45 minutes. The supernatant was decanted and saved. The following steps involved further purifying the protein. A volume of 15 ml solution of 10% Triton-X was added to the pellet and incubated at room temperature for 10 mins. The re-suspended pellet was centrifuged at 4°C at 3000 rpm for 20 minutes. The supernatant was decanted as previously stated. A volume of 15 ml of 1% Triton-X was added to the pellet. A stirring rod was used to dissolve the pellet and incubated at room temperature for 10 mins. The re-suspended pellet was centrifuged at 4°C at 3000 rpm for 20 minutes. The supernatant was decanted as

previously stated. This step was repeated. The pellet was dissolved in 15 ml of His-Tag binding buffer with 6 M urea added. Then, the solution was placed in the cold room overnight with a stir bar.

To further purify NCAD12-P16A using solvents with different binding affinities, His-tag chromatography was used. The solution was centrifuged at 4°C at 3000 rpm for 20 minutes. The supernatant was save because it contained the protein that would be used on the His-tag column. Before the column could be used, it had to be equilibrated by running 25 ml of 6 M Urea Binding Buffer through the column. Once this was completed, 5 ml of the protein was loaded into the column and the flow through was collected. Next, 5 ml of His-tag binding buffer was loaded onto the column and the flow through was collected (~5 ml increments). This step was repeated three more times. Then, 20 ml of wash buffer was loaded onto the column and the flow through was collected (~5 ml increments). Finally, 30 ml of elution buffer was loaded onto the column and the flow through was collected (~5 ml increments). This entire process was repeated for the remainder of the crude protein sample. In order to determine which His-tag fractions contained protein, the absorbance (at 280 nm) of each fraction was taken after being blanked against the appropriate buffer.

The Elution Buffer fractions with the highest absorbance were combined into one sample. The sample was dialyzed in trypsin digest buffer to equilibrate the protein via buffer exchange for ideal conditions for trypsin digestion. The sample was placed into a 12 cm molecular porous membrane, which was clipped at both ends. Membranes were then immersed in 2 L of Trypsin Digest Buffer (140 mM NaCl, 20 mM Tris, 10 mM CaCl₂, 1 mM DTT, and 5% glycerol, pH 7.9) with a stir bar on speed 3 and placed in the cold room overnight (covered with aluminum foil). The sample was removed and placed into a conical. Eight micro-centrifuge tubes were labeled (1-

8). To each tube, 250 ul of immobilized trypsin and 750 ul of trypsin dialyzed protein were added. The tubes were vortexed and centrifuged for 5 mins at room temperature. The supernatant was decanted, and the process was repeated two more times. Next, the digested protein was dialyzed in 500 ml of SEC buffer (10 mM HEPES, 140 mM NaCl, pH 7.4). The buffer was changed every 2 hours to ensure buffer exchange happened between trypsin digestion and the standard apo-buffer which will be used in future studies. After dialysis, the protein concentration (~38 uM) was determined by checking the absorbance, using UV-vis spectroscopy, at 280nm ($\epsilon_{280} = 15,900 \pm 400 \text{ M}^{-1}\text{cm}^{-1}$)⁴⁷. The protein was then aliquoted into 1.5 ml micro-centrifuge tube and frozen for later use.

THERMAL DENATURATION

Thermal denaturation was monitored by AVIV 202SF circular dichroism (CD) spectrometer. To determine the stability of NCAD12-P16A, a 1:20 dilution was made from the protein sample to obtain a protein concentration of 5 μM . The sample was placed in a 1 cm quartz cuvette and a spectrum (300 to 200nm) was taken using UV-vis spectroscopy. A small stir bar was added to the sample and the sample was placed in CD. The temperature probe was added and a spectrum was taken to ensure the protein signal was apparent and the temperature probe did not interfere with the light source. The optimum wavelength for monitoring thermal denaturation was 227 nm. The temperature ramp was 1°C/min with a 30 second to 1 min equilibration time with a 5 sec acquisition time at 230 nm. The temperature varied from 15°C to 95°C. All thermal unfolding transitions were fit to the Gibbs Helm Holtz equation, which is:

$$\Delta G = \Delta H_m \left(1 - \frac{T}{T_m}\right) + \Delta C_p \left(T - T_m - T \ln \frac{T}{T_m}\right) \quad (1)$$

where ΔH_m is the enthalpy of unfolding at the melting temperature, and ΔC_p is the heat capacity change for denaturation. The value of ΔC_p was fixed to 1 kcal/molK in all fits. ΔG is the calculated free energy at 25°C based on resolved parameters.

CALCIUM BINDING

Calcium titrations of NCAD12-P16A were monitored by circular dichroism (CD) and fluorescence (FL) spectroscopy. The titrations were performed on protein concentrations of 5 μ M in SEC buffer with a total volume of ~2000 μ l. The titrations monitored by CD were done in a 1 cm cuvette with a stirring by adding small volumes (2.5 μ l, 5 μ l, and 10 μ l) of calcium chloride stocks of different concentrations (1 μ M, 10 μ M, 100 μ M, 1M). After the calcium addition was made, spectra were taken from 220 to 300 nm with 5 sec averaging time. Each titration was performed in triplicate. CD data at wavelengths between 225 and 235 were processed and analyzed as individual titration curves. A second set of identical titrations was also monitored by fluorescence emission (FL). The protein solutions were prepared at 5 μ M total protein concentration and titrated as mentioned previously. Emission spectra were recorded from 300 to 425 nm with excitation wavelength set at 280 nm. The data from the CD and FL titration were fit individually to the Adair equation to resolve the free energy change of calcium binding as shown below in Eq 2:

$$\bar{Y} = \frac{K_a X}{1 + K_a X} ; K_a = \exp\{-\Delta G^\circ/RT\} \quad (2)$$

where \bar{Y} is the fractional saturation of sites and K_a is the calcium association constant. These experiments will yield estimates of the midpoint of the calcium binding titrations.

CHAPTER III

RESULTS

PROTEIN EXPRESSION

The SDS-PAGE gel (**Figure 4**) shows the complete sequence of steps for the expression and purification of NCAD P16A. There is a clear expression of the recombinant protein that is a dominant band at ~30 kDa. Contamination bacterial proteins are obvious at higher and lower molecular weights. Lane 3 shows the effectiveness of the triton-x washes, which effectively reduce the levels of contaminating bacterial bands. Some lower molecular weight fragments are formed upon digestion of protein in trypsin to remove the 45 aa N-terminal extension. The relative concentration of expressed protein increased as the purification process progressed. The overall molecular weight of NCAD P16A is ~25 kDa. The sample in lanes 6 and 7 represents the purity of the protein used throughout the expression and purification process.

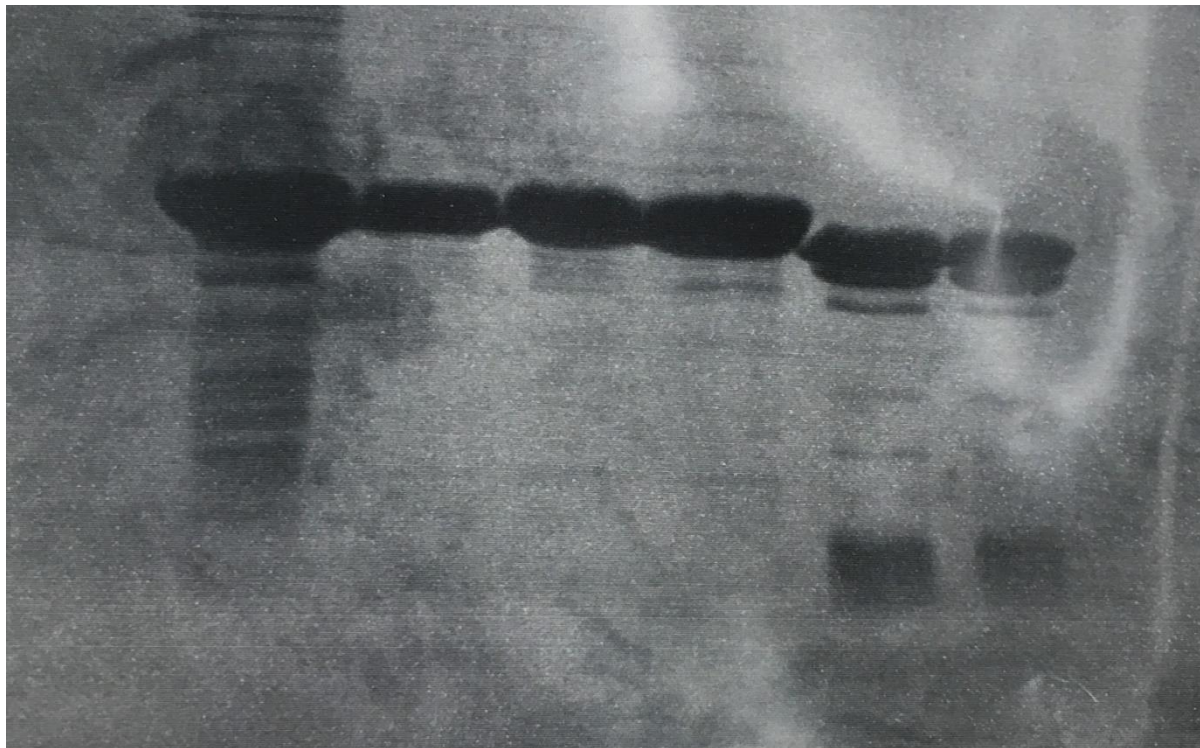


Figure 4: 17% SDS-PAGE of Protein Expression and Purification. Lanes 1-7 represent the various steps of the protein expression and purification. Lane 1 is the standard protein ladder. Lane 2 is the pre-his tag sample that was dialyzed in Binding Buffer overnight. Lane 3 is the post-his tag sample that was dialyzed in Binding Buffer overnight. Lane 4 is the combines post-his tag fractions. Lane 5 is the pre trypsin dialysis. Lanes 6 and 7 are the post trypsin digestion of samples.

THERMAL DENATURATION

Thermal denaturations of NCAD12 and P16A were monitored by AVIV 202SF spectrometer. CD signal at 227 nm was measured as a function of temperature which scanned from 15°C to 95°C. The experiments were performed using a quartz cuvette with a 1 cm path covered with a temperature probe top. Each sample contained 5 μ M of protein with a specific amount of SEC buffer for a total volume of 2000 μ L of sample. Before data were acquired at each temperature, there was a 1 min equilibration time to stabilize the temperature. For both proteins (**Figures 6 and 7**) dependent and independent variables as the temperature increased, the protein

unfolded and the CD signal decreased. In NCAD12 and P16A, there was a midpoint of $\sim 40^{\circ}\text{C}$ for the first transition. The second transition had a drifting signal with an unclear unfolded baseline and a midpoint of $\sim 60^{\circ}\text{C}$.

The first transitions of each protein were fit to the Gibbs Helmholtz equation with linear folded and unfolded baselines. The baselines contained adjustable slopes and intercepts. The ΔC_p was fixed to 1 kcal/Kmol. Quantitative analysis was performed on the first transition ~ 40 data points. The resolved parameters are listed in **Table 2**. Global Analysis was performed to fit the thermal denaturations for P16A and NCAD12 into a single curve fit. There was a slight decrease in P16A compared to NCAD12 $\Delta H_m \sim 13$ kcal/mol, $T_m \sim 6^{\circ}\text{C}$, and ΔG° at $37^{\circ}\text{C} \sim 1.6$ kcal/mol. The $\sim 6^{\circ}\text{C}$ difference in T_m is significant. Loss of Pro16 (loss of conformational restriction) decreased stability of EC2 (transition 1) by ~ 1 kcal/mol (25%).

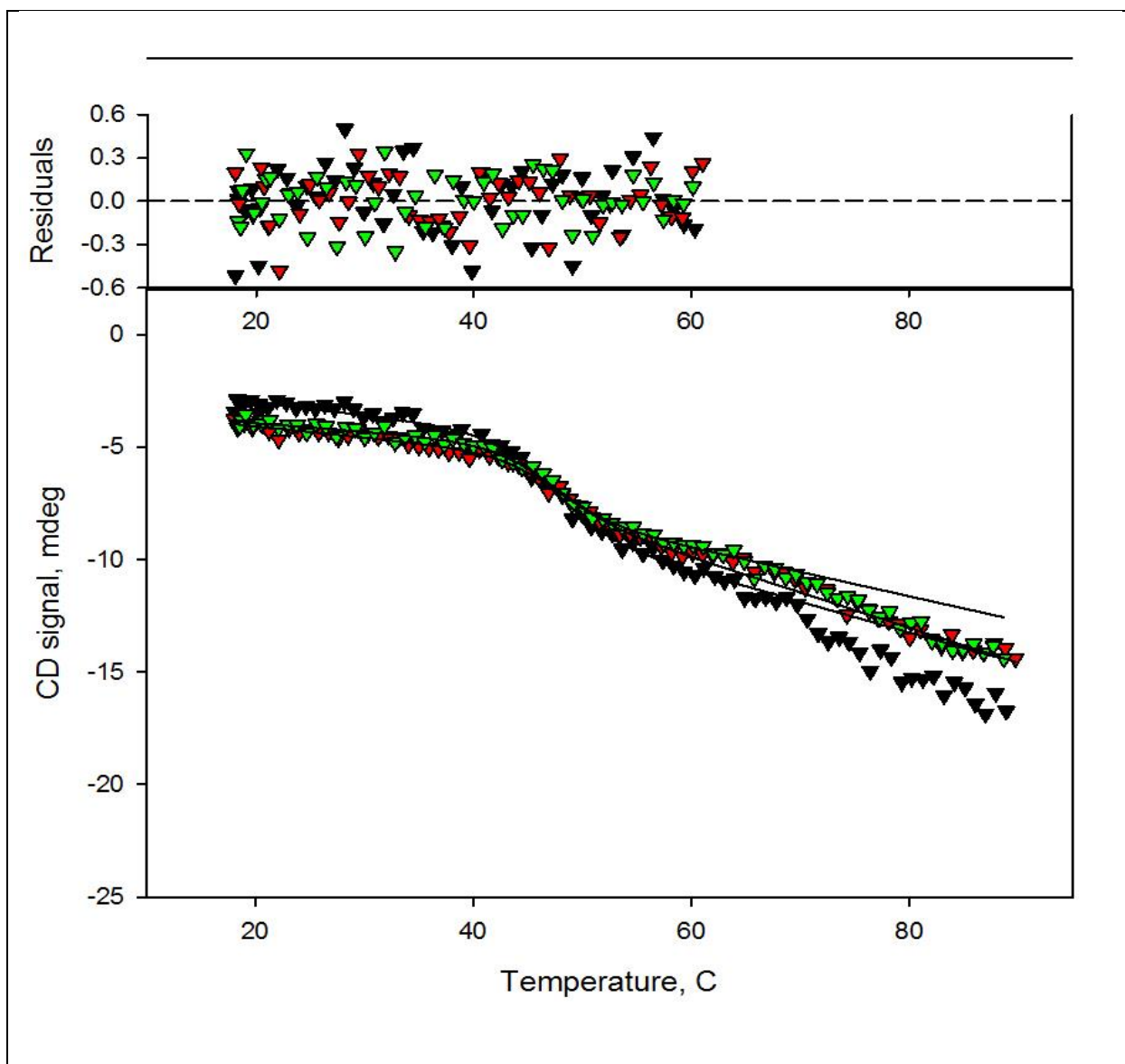
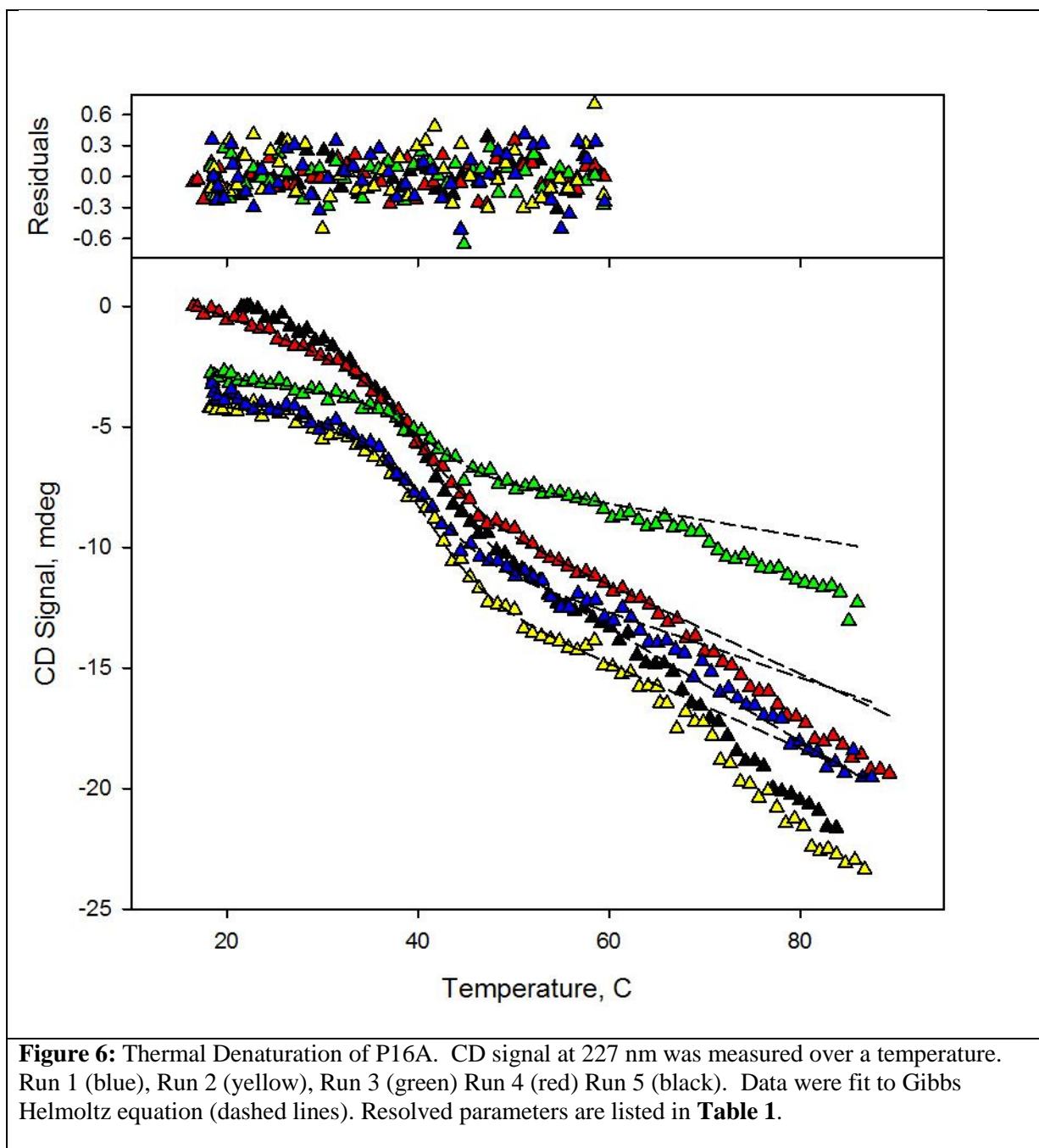


Figure 5: Thermal Denaturation of NCAD12. CD signal at 227 nm was measured over a temperature. Run 1 (green), Run 2 (red), Run 3 (black). Data were fit to Gibbs Helmholtz equation (solid lines). Resolved parameters are listed in **Table 1**.



	ΔH_m (kcal/mol)	T_m (°C)	ΔC_p (kcal/mol)	ΔG° (25°C) (kcal/mol)
Wild Type (n=3)	72 ± 8	46.6 ± 0.7	1 ± 0	4.1 ± 0.9
P16A (n=5)	59 ± 4	40.1 ± 0.3	1 ± 0	2.5 ± 0.4

Table 2: Resolved parameters. Data fitted to the Gibbs Helm Holtz equation. Reported errors were resolved from a global analysis of replicate experiments.

CALCIUM TITRATIONS

The calcium-dependent changes in spectra of CD and FL were monitored during calcium titrations. **Figures 8** and **9** represent the CD and FL signals as a function of total calcium concentration. The spectral data at each point were corrected for offset to reduce scatter in the final titration data. The CD and FL signals increased (became less negative) with the addition of calcium. Based on the randomness and span of residuals, data fitted well to a binding model of equal and independent sites indicating that there was no observed cooperativity in calcium binding. The ΔG° values for CD and FL (**Table 2**) are very similar. There is a slight ΔG° increase of 0.1 (kcal/mol) in CD compared to FL.

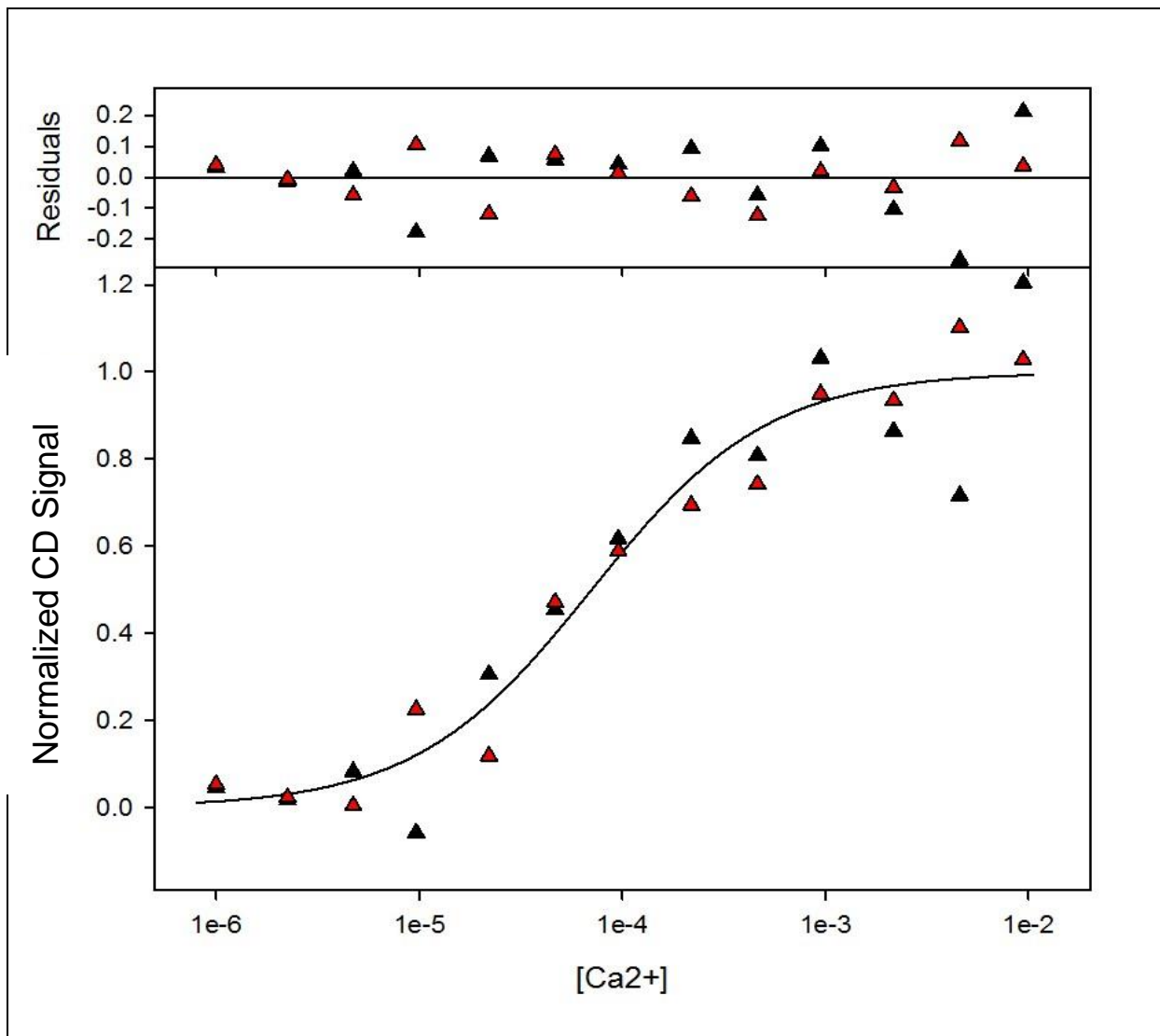


Figure 7: Calcium Titration of P16A monitored by CD. Run 1 (red) and Run 2 (black). The CD signal is plotted against total calcium concentration. Solid line is simulated based of parameters resolved from global analysis of at least two separate experiments. Resolved values for the change in free energy of binding are shown in **Table 2**.

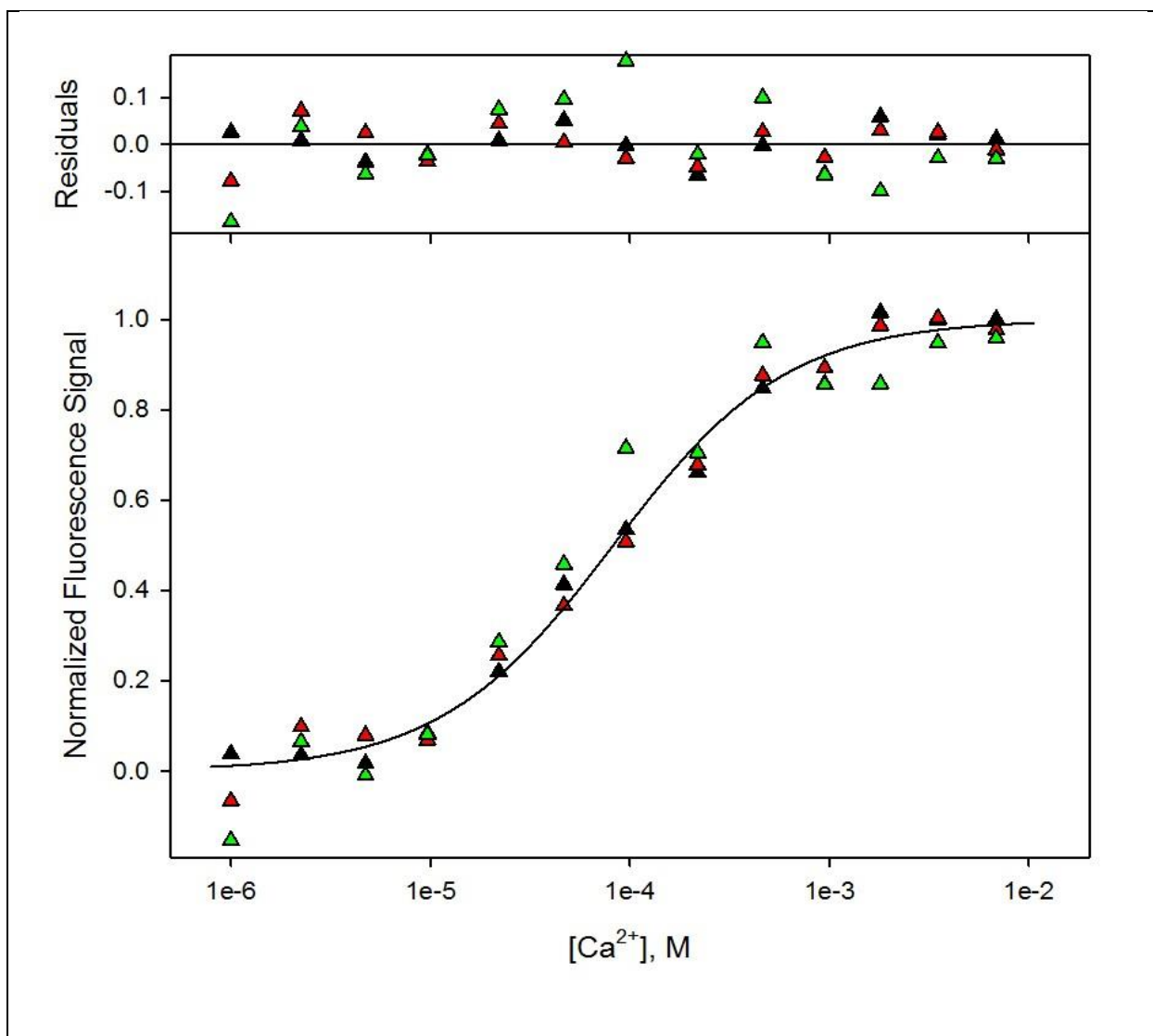


Figure 8: Calcium Titration of P16A on FL. Run 1 (green), Run 2 (red), and Run 3 (black). The CD signal is plotted against total calcium concentration. Solid line is simulated based of parameters resolved from global analysis of at least two separate experiments. Resolved values for the change in free energy of binding are shown in **Table 2**.

	P16 A CD (n=2)	P16 A FL (n=3)	NCAD12
ΔG° (kcal/mol)	-5.7 ± 0.2	-5.6 ± 0.1	-----
K_a	1.53×10^4	1.29×10^4	$3.5 \pm 1.0 \times 10^4$

Table 3: Free Energies of Calcium Binding Resolved from Global Analysis of Calcium Titrations. Data were fit to the Adair equation. Reported errors were resolved from a global analysis of replicate experiments. ΔG° values were calculated at 25°C. The K_a values were compared to that of NCAD12 from the literature ⁴⁸.

CHAPTER IV

DISCUSSION

A focal point of the research in the Pedigo laboratory has been to find a molecular mechanism that explains the striking difference in the calcium-dependent kinetics of dimerization of ECAD and NCAD. Discussions in the field have been dominated by an intriguing X-dimer structure that may be the transition state structure between the closed monomer and closed dimer forms ²⁶. After investigation, it was determined that if an X-dimer type intermediate exists for NCAD, it does not require R14 for rapid monomer dimer exchange. However, dimer exchange kinetics are greatly impaired by a glutamate in position 14 ^{26-28,45}. The sensitivity to the acidic residue in position 14 drew our attention to this regions of the proteins, a connecting region between the E11, a chelating residue for calcium, and N20, the first amino acid of the β B-strand. Our attention was drawn to P16, a notable difference between NCAD and ECAD. Perhaps this residue plays a role in the differences in dimerization kinetics between NCAD and ECAD.

The purpose of these studies were to understand the impact P16A mutation has on the stability and calcium binding affinity of NCAD12. Proline is a conformationally restricted amino acid. By mutating it to an alanine, an amino acid with less restriction, we expected to observe differences in the stability and calcium binding affinity compared to NCAD12. From the results of these studies, we would infer the role of P16 in the wild type protein. Thermal denaturation studies observed the stability of P16A in the apo state, allowing us to assess whether the mutation destabilized the folded structure. In addition, denaturation studies ensured that the protein was

stable and behaved in an expected way in order to obtain meaningful calcium binding data. Calcium binding studies report the impact of the P16A mutation on the binding affinity. Since the protein must be folded and bind calcium in order to form dimer, then both the stability and calcium binding affinity will affect dimerization affinity and kinetics.

THERMAL DENATURATION

Thermal denaturation studies show that there is a decrease in the protein stability of P16A compared to wild type NCAD12. We assume that the protein is in its natively folded state before heat is applied. As more heat is applied, the protein unfolds. Previous studies have shown that EC2 domain (~40°C) unfolds before EC1 domain (~70°C) for both NCAD and ECAD³⁴. There are two transitions observed in each graph (**Figures 5 and 6**). As signal increased, there was a decrease in temperature. The first transition, unfolding of EC2, has a distinct cooperative unfolding transition that appears to be completed before the second transition is observed (unfolding of EC1). The second transition, unfolding of EC1, has an uncooperative unfolding transition. It shifts to a higher temperature which indicates that there is an order to which unfolding of each domain occurs and EC1 unfolds after EC2.

Although the P16A mutation is located in EC1, it has an overall effect on the stability of EC2. This trend can also be seen in the E89A mutation in EC1 of NCAD12³⁴⁻³⁶. In order to analyze just the unfolding of EC2, data have to be truncated in order to resolve the thermodynamic parameters for EC2. Fitting of unfolding data for EC1 in NCAD12 is problematic because of the absence of a well resolved unfolded baseline. The T_m for P16A is ~40.1°C. This T_m value lies directly between NCAD12 (~46.6°C) and ECAD12 (~33.7°C)³⁷. The ΔG° for NCAD12 P16A is 2.5 ± 0.4 kcal/mol. This ΔG° value is more comparable to that of ECAD12 (1.9 ± 0.3 kcal/mol) than NCAD12 (4.1 ± 0.9 kcal/mol) which has a two times higher affinity. Overall, NCAD P16A

destabilizes the stability of NCAD12 in terms of T_m and ΔG° values. In conclusion, the P16A mutation in NCAD12 spans about half the differences in the biophysical parameters between NCAD12 and ECAD12. One can conclude that the P16 is an important determinant of the differences in the stability of ECAD and NCAD, but only part of the difference.

CALCIUM BINDING

The effect of P16A on calcium binding affinity showed that P16A has a lower binding constant compared to that of NCAD12. This is shown by observing the K_a values. P16A ($1.5 \pm 1.1 \times 10^4$) is roughly two folds lower than NCAD ($3.5 \pm 1.0 \times 10^4$). The data was fit to an equal independent model. Based on the residuals, the model happened to be a good fit due to the randomness of the data. This can also be seen in the data points following the sigmoidal curve trend. One can conclude that calcium binds at a slower rate in P16A than NCAD12.

Additional studies were performed with analytical size exclusion chromatography to compare the dimerization kinetics, K_d value, of NCAD and P16A. In the protein solution, there exists monomer and dimer. From this, we can observe the rate of monomer and dimer exchange. P16A had a K_d value of $77 \mu\text{M}$, which is compared to the NCAD12 K_d value of $25 \mu\text{M}$. P16A has a three-fold lower dimerization affinity than NCAD. P16A dimerizes at a slower rate than NCAD12, which makes it more comparable to ECAD ($K_d = 100 \mu\text{M}$).

By using thermal denaturation and calcium binding studies, it appears that P16A is less stable and has a lower calcium binding affinity than NCAD12. In comparison of NCAD12 and P16A with analytical size exclusion chromatography, P16A also lowers the dimerization of NCAD. Overall, P16A has a significant effect on NCAD12. Further studies are needed to examine the kinetic effects of P16A compared to NCAD12 through other analytical SEC studies and with other mutants such as P16E, a mutant that would convert NCAD to ECAD at that site. These

studies would provide information on the role of P16 in the kinetics and equilibria of dimerization in NCAD12. Currently, these experiments are being studied in Dr. Pedigo's lab.

BIBLIOGRAPY

1. Buckley, Christopher D., et al. "Cell adhesion: more than just glue (review)." *Molecular membrane biology* 15.4 (1998): 167-176.
2. Koch, Peter J., and Werner W. Franke. "Desmosomal cadherins: another growing multigene family of adhesion molecules." *Current opinion in cell biology* 6.5 (1994): 682-687.
3. Magee, Anthony I., and Roger S. Buxton. "Transmembrane molecular assemblies regulated by the greater cadherin family." *Current opinion in cell biology* 3.5 (1991): 854-861.
4. Alattia, J. R., H. Kurokawa, and M. Ikura. "Structural view of cadherin-mediated cell-cell adhesion." *Cellular and Molecular Life Sciences CMLS* 55.3 (1999): 359-367.
5. Gumbiner, Barry M. "Cell adhesion: the molecular basis of tissue architecture and morphogenesis." *Cell* 84.3 (1996): 345-357.
6. Briehner, William M., Alpha S. Yap, and Barry M. Gumbiner. "Lateral dimerization is required for the homophilic binding activity of C-cadherin." *The Journal of Cell Biology* 135.2 (1996): 487-496.
7. Takeichi, Masatoshi. "Cadherin cell adhesion receptors as a morphogenetic regulator." *Science* 251.5000 (1991): 1451-1455.
8. Tepass, Ulrich, et al. "Cadherins in embryonic and neural morphogenesis." *Nature Reviews Molecular Cell Biology* 1.2 (2000): 91-100.
9. Larue, Lionel, et al. "E-cadherin null mutant embryos fail to form a trophectoderm epithelium." *Proceedings of the National Academy of Sciences* 91.17 (1994): 8263-8267.

10. Tang, Lixin, Chou P. Hung, and Erin M. Schuman. "A role for the cadherin family of cell adhesion molecules in hippocampal long-term potentiation." *Neuron* 20.6 (1998): 1165-1175.
11. Berx, Geert, et al. "Mutations of the human E-cadherin (CDH1) gene." *Human mutation* 12.4 (1998): 226.
12. Berx, Geert, Friedel Nollet, and Frans Van Roy. "Dysregulation of the E-cadherin/catenin complex by irreversible mutations in human carcinomas." *Cell Communication & Adhesion* 6.2-3 (1998): 171-184.
13. Bussemakers, Marion JG, et al. "Decreased expression of E-cadherin in the progression of rat prostatic cancer." *Cancer research* 52.10 (1992): 2916-2922.
14. González-Mariscal, Lorenza, et al. "Tight junctions and the regulation of gene expression." *Seminars in cell & developmental biology*. Vol. 36. Academic Press, 2014.
15. Chothia, Cyrus, and E. Yvonne Jones. "The molecular structure of cell adhesion molecules." *Annual review of biochemistry* 66.1 (1997): 823-862.
16. Ozawa, Masayuki, Helene Baribault, and Rolf Kemler. "The cytoplasmic domain of the cell adhesion molecule uvomorulin associates with three independent proteins structurally related in different species." *The EMBO Journal* 8.6 (1989): 1711.
17. Fujiyama, F., Stephenson, F. A., and Bolam, J. P., Synaptic localization of GABA(A) receptor subunits in the substantia nigra of the rat: effects of quinolinic acid lesions of the striatum, *Eur J Neurosci*, 15, 1961 (2002).
18. Knott, G. W., Quairiaux, C., Genoud, C., and Welker, E., Formation of dendritic spines with GABAergic synapses induced by whisker stimulation in adult mice, *Neuron*, 34, 265 (2002).

19. Pearson, W., LALIGN - find multiple matching subsegments in two sequences (2009).
20. Katsamba, P., et al. "Linking molecular affinity and cellular specificity in cadherin-mediated adhesion." *Proceedings of the National Academy of Sciences* 106.28 (2009): 11594-11599.
21. Tamura, K., et al., Structure-function analysis of cell adhesion by neural (N-) cadherin. *Neuron*, 1998. 20(6): p. 1153-63.
22. Pertz, O., et al., A new crystal structure, Ca²⁺ dependence and mutational analysis reveal molecular details of E-cadherin homoassociation. *Embo J*, 1999. 18(7): p. 173847.
23. Perret, E., et al., Fast dissociation kinetics between individual E-cadherin fragments revealed by flow chamber analysis. *Embo J*, 2002. 21(11): p. 2537-46.
24. Harrison, Oliver J., et al. "The extracellular architecture of adherens junctions revealed by crystal structures of type I cadherins." *Structure* 19.2 (2011): 244-256.
25. Vunnam, Nagamani, et al. "Dimeric states of neural-and epithelial-cadherins are distinguished by the rate of disassembly." *Biochemistry* 50.14 (2011): 2951-2961.
26. Harrison, Oliver J., et al. "Two-step adhesive binding by classical cadherins." *Nature structural & molecular biology* 17.3 (2010): 348-357.
27. Vunnam, Nagamani, and Susan Pedigo. "X-interface is not the explanation for the slow disassembly of N-cadherin dimers in the apo state." *Protein Science* 21.7 (2012): 1006-1014.
28. Vunnam, Nagamani, Nathan I. Hammer, and Susan Pedigo. "Basic residue at position 14 is not required for fast assembly and disassembly kinetics in neural cadherin." *Biochemistry* 54.3 (2015): 836-843.

29. Betts, Matthew J., and Robert B. Russell. "Amino acid properties and consequences of substitutions." *Bioinformatics for geneticists* 317 (2003): 289.
30. Wedemeyer, William J., et al. "Disulfide bonds and protein folding." *Biochemistry* 39.15 (2000): 4207-4216.
31. Green, Susan M., et al. "One-step evolution of a dimer from a monomeric protein." *Nature Structural & Molecular Biology* 2.9 (1995): 746-751.
32. Schultz, David A., and Robert L. Baldwin. "Cis proline mutants of ribonuclease AI Thermal stability." *Protein Science* 1.7 (1992): 910-916.
33. Miller, Katherine H., Jessica R. Karr, and Susan Marqusee. "A hinge region cis-proline in ribonuclease A acts as a conformational gatekeeper for C-terminal domain swapping." *Journal of molecular biology* 400.3 (2010): 567-578.
34. Vunnam, Nagamani, and Susan Pedigo. "Prolines in β A-sheet of neural cadherin act as a switch to control the dynamics of the equilibrium between monomer and dimer." *Biochemistry* 50.32 (2011): 6959-6965.
35. Vendome, Jeremie, et al. "Molecular design principles underlying β -strand swapping in the adhesive dimerization of cadherins." *Nature structural & molecular biology* 18.6 (2011): 693-700.
36. Vunnam, Nagamani, and Susan Pedigo. "Sequential binding of calcium leads to dimerization in neural cadherin." *Biochemistry* 50.14 (2011): 2973-29
37. Prasad, Alka, et al. "Effect of linker segments on the stability of epithelial cadherin domain 2." *Proteins: Structure, Function, and Bioinformatics* 62.1 (2006): 111-121.
38. Prakasam, A., et al. "Calcium site mutations in cadherin: impact on adhesion and evidence of cooperativity." *Biochemistry* 45.22 (2006): 6930-6939.

39. Hazan, Rachel B., et al. "Exogenous expression of N-cadherin in breast cancer cells induces cell migration, invasion, and metastasis." *The Journal of cell biology* 148.4 (2000): 779-790.
40. Uemura, Tadashi. "The cadherin superfamily at the synapse: more members, more missions." *Cell* 93.7 (1998): 1095-1098.
41. Ozawa, Masayuki. "Lateral dimerization of the E-cadherin extracellular domain is necessary but not sufficient for adhesive activity." *Journal of Biological Chemistry* 277.22 (2002): 19600-19608.
42. Shapiro, Lawrence, et al. "Structural basis of cell-cell adhesion by cadherins." *Nature* 374.6520 (1995): 327-337.
43. Boggon, Titus J., et al. "C-cadherin ectodomain structure and implications for cell adhesion mechanisms." *Science* 296.5571 (2002): 1308-1313.
44. Parisini, Emilio, et al. "The crystal structure of human E-cadherin domains 1 and 2, and comparison with other cadherins in the context of adhesion mechanism." *Journal of molecular biology* 373.2 (2007): 401-411.
45. Hong, S., Troyanovsky, R. B., and Troyanovsky, S. M. (2011) Cadherin exits the junction by switching its adhesive bond. *J Cell Biol* 192, 1073-1083.
46. Vunnam, Nagamani, and Susan Pedigo. "Calcium-induced strain in the monomer promotes dimerization in neural cadherin." *Biochemistry* 50.39 (2011): 8437-8444.
47. Edelhoch, Harold. "Spectroscopic determination of tryptophan and tyrosine in proteins*." *Biochemistry* 6.7 (1967): 1948-1954.
48. Jungles, Jared M., et al. "Impact of pH on the Structure and Function of Neural Cadherin." *Biochemistry* 53.47 (2014): 7436-7444.

VITA

EDUCATION

BS in Chemistry Jackson State University April 2012